PRESENTATION TITLE

Motion model and super-resolution reconstruction from multi-slice MR image data using an MR-derived surrogate

AUTHOR(S)

Björn Eiben[1*], Elena H. Tran[1], Andreas Wetscherek[2], Uwe Oelfke[2], David J. Hawkes[1], and Jamie R. McClelland[1]

[1] *Centre for Medical Image Computing, Dept. of Medical Physics and Biomedical Engineering, University College London, UK*

[2] *Joint Department of Physics, The Institute of Cancer Research and The Royal Marsden NHS Foundation Trust, London, UK*

ABSTRACT

Purpose: Respiratory motion models have the potential to take on an important role in MR-guided radiotherapy of lung cancer patients for offline dose reconstruction, planning, adaptive treatment, and tracked treatment since they provide detailed spatiotemporal information about the patient. However, most motion modelling approaches rely on temporally resolved image volumes to estimate the 3D motion. The formation of such volumes assumes regular motion, which can lead to artefacts in the images, or requires very long acquisitions to sample the motion fully. To avoid using pre-sorted data, we propose using a generalised motion modelling framework that directly optimises the motion model parameters on the unsorted partial image data, in this case the individual slices from a multi-slice acquisition. Furthermore, our modelling framework allows integration of super-resolution motion-compensated image reconstruction, hence outputs both a 'motion free' 3D volume and a motion model that estimates the 3D motion from the surrogate signal(s). Here, for the first time, we apply this framework using an MR-derived surrogate signal and multi-slice MR image data acquired in both sagittal and coronal orientations.

Materials & Methods: Image slices of the thorax were acquired from a volunteer on a Siemens Aera 1.5T scanner using a gradient echo sequence (TE/TR=2.1/4.2ms), and a resolution of 2x2x10mm^3. The model slices (used to fit the model) were interleaved with sagittal surrogate slices from a fixed position in the centre of the right lung. Two surrogate signals were generated by applying PCA to the deformation fields resulting from registering the surrogate slices. The model slices were acquired in coronal and sagittal orientations. The slice spacing was 2mm, so there was an 8mm overlap between adjacent slices, facilitating the super-resolution reconstruction. Each model slice was acquired ten times, resulting in 2800 model and surrogate slices each. The reconstructed volume had a resolution of 2x2x2mm^3. To measure the improvement in image quality due to the motion model, we generated an additional super-resolution image without using motion compensation, as well as the motion compensated image resulting from the application of our framework. We measured the improvement in image sharpness by comparing exemplary intensity profiles at the diaphragm-lung boundary in terms of a fitted density function and the sigma value of the associated Gaussian distribution.

Results: Figure 1 shows the non-motion compensated (a)-(c) and motion compensated (e)-(g) reconstructed volumes. Sigma of the density function fitted to the intensity profiles decreased from 5.5 to 1.0mm (Fig.1 (d,h)). Furthermore, the motion compensated image volume was animated using the fitted motion model and corresponding input surrogate signal. We found a good visual agreement between the individual model slices and the deformed reconstructed image. The animated motion appeared plausible throughout the field of view with minor artefacts associated with sliding motion between the lungs and rib cage.

Conclusions: We present a feasibility study that successfully applied our unified motion modelling framework to build a volumetric motion model from partial image data and simultaneous reconstruct a coherent image volume while using an MR-derived surrogate signal.

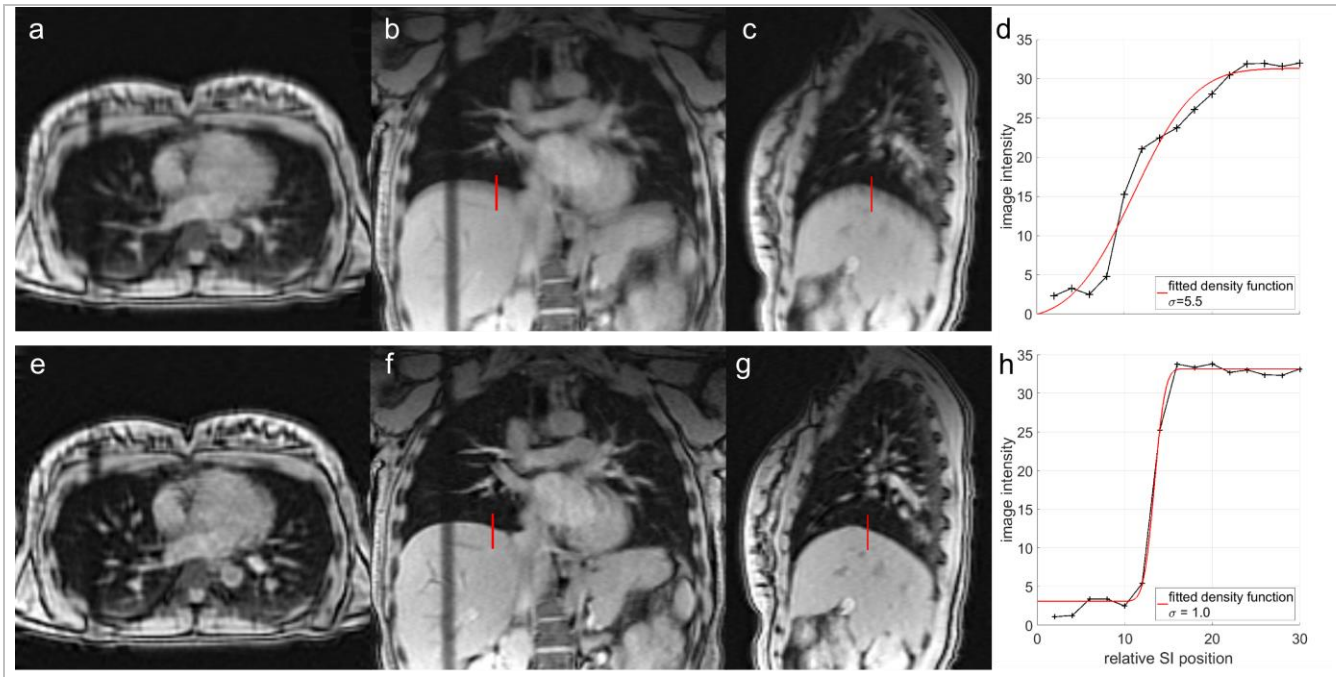

Fig. 1 *Reconstructed image volumes without motion compensation (a)-(c), and with motion compensation (e)-(g). Both images were reconstructed to an isotropic resolution of 2mm. Line profile locations are indicated in red with corresponding line profiles and fitted density functions plotted in subfigures (d) and (h).*